<100 ppm show an almost constant N abundance signature, irrespective of the concentrations, with $\delta^{15}N \approx -15 \pm 15‰$. There are two major sources for the analytical blank: outgassing of the sample chamber and sample surface contamination. Only the outgassing N is corrected here. This correction represents <1% of the N concentrations and only a few ‰ of the extreme $\delta^{15}N$ values measured in the first few tens of nm of the grains. At >150-nm depth of the grain, blank (outgassing) N often accounts for ~50% of the detected N, although the exact fraction varies, depending on the analytical condition, such as the sputtering rate or the rastering size. (For the correction for the outgassing N, we adopt the minimum amount among the possible range to avoid overcorrection of the blank.) Degrees of surface contamination are largely variable, depending on grains. The surface contamination is observed prominently at <50-nm depth. Its concentration at the most surface of the sample (when the primary ion beam crosses the border of the gold film and the sample) normally ranges from 100 to 5000 ppm. No systematic difference is observed in the contamination level between the grains in samples 71501 and 79035 or between ilmenite and silicate grains.

20. The δD values of sample 71501 corrected for cosmogenic D ($\delta D_{trapped}$), assuming a maximum exposure age of 200 Ma (*11*) and using a D production rate [L. Merlivat, M. Lelu, G. Nief, E. Roth, *Proc. Lunar Sci. Conf.* **VII**, 649 (1974)], are available at *Science* Online (*18*). The amount of cosmogenic D relative to implanted H in grain 1 from sample 79035 is negligible.
21. The best estimate for the minimum $\delta^{15}N$ value observed in grain 1 from sample 79035 ($-240 \pm 25‰$) is obtained from the weighted average, taken from $\delta^{15}N$ values as low as –200‰. Though lower values are observed, e.g., $-290 \pm 100‰$ (*18*) at 120-nm depth (Fig. 1A), the differences from the best estimate value are not significant. The observed $\delta^{15}N$ value (–240‰) can be regarded as the upper limit for the SW $\delta^{15}N$ value, because the observed values are not perfectly free of blank N, especially the surface contamination N.
22. R. Wieler, H. Baur, *Astrophys. J.* **453**, 987 (1995).
23. L. P. Keller, D. S. McKay, *Geochim. Cosmochim. Acta* **61**, 2331 (1997).
24. J.-P. Benkert, H. Baur, P. Signer, R. Wieler, *J. Geophys. Res.* **98**, 13147 (1993).
25. P. Bochsler, R. Kallenbach, *Meteoritics* **29**, 653 (1994).
26. F. Humbert, thesis, Université Henri Poincaré, Nancy 1, France (1998).
27. J. Geiss, G. Gloeckler, R. von Steiger, *Philos. Trans. R. Soc. London A* **349**, 213 (1994).
28. R. Kallenbach *et al.*, *Astrophys. J.* **507**, L185 (1998).
29. T. Fouchet *et al.*, *Icarus* **143**, 223 (2000).
30. E. Zinner, *Annu. Rev. Earth Planet. Sci.* **26**, 147 (1998).
31. M. B. McElroy, Y. L. Yung, A. O. Nier, *Science* **194**, 70 (1976).
32. Assuming that N is lost from a N-bearing host phase with a rate proportional to the inverse square root of the atomic mass ($m^{-1/2}$), 4.5 or 18 orders of magnitude depletion of N concentration is required to enrich ^{15}N by 40 or 300%, respectively, from the initial isotopic composition. To explain by such fractionation the N isotopic composition of CI chondrites, which is enriched in ^{15}N by 40% relative to the solar value, the initial N concentration must be about three orders of magnitude overabundant in comparison to the solar composition (because the N/major solid elements ratio in CI chondrites is 1.7 orders of magnitude lower than the solar value), which is highly unrealistic.
33. N. G. Adams, D. Smith, *Astrophys. J.* **247**, L123 (1981).
34. Ratios averaged over wide depth ranges, rather than H and N isotopic compositions observed at respective depths, are plotted in Fig. 2. This is because the latter may not always reflect the original mixing proportion of the SW and nonsolar components when they were acquired, because H in the present grain is not located at the original site but is diffused over a long range within the grains.
35. B. Marty, L. Zimmermann, *Geochim. Cosmochim. Acta* **63**, 3619 (1999).
36. D. C. Jewitt, H. E. Matthews, T. Owen, R. Meier, *Science* **278**, 90 (1997).
37. Samples were provided by NASA. We thank R. Wieler for constructive comments and suggestions, H. Fukui and O. Ohtaka for preparing the synthetic glass standards, and N. Shimobayashi and M. Kitamura for nondestructive elemental mapping of lunar grains. K.H. thanks members of CRPG-CNRS for their hospitality during his stay. This study was supported by the Japanese Ministry of Education, Science, Sports and Culture and by CNRS through a "Poste Rouge" fellowship by grants from Institut National des Sciences de l'Univers–Programme, National de Planétologie and from Région Lorraine (K.H.). This work is CRPG-CNRS contribution 1488.

3 August 2000; accepted 29 September 2000

Decadal Sea Surface Temperature Variability in the Subtropical South Pacific from 1726 to 1997 A.D.

Braddock K. Linsley,[1] Gerard M. Wellington,[2] Daniel P. Schrag[3]

We present a 271-year record of Sr/Ca variability in a coral from Rarotonga in the South Pacific gyre. Calibration with monthly sea surface temperature (SST) from satellite and ship measurements made in a grid measuring 1° by 1° over the period from 1981 to 1997 indicates that this Sr/Ca record is an excellent proxy for SST. Comparison with SST from ship measurements made since 1950 in a grid measuring 5° by 5° also shows that the Sr/Ca data accurately record decadal changes in SST. The entire Sr/Ca record back to 1726 shows a distinct pattern of decadal variability, with repeated decadal and interdecadal SST regime shifts greater than 0.75°C. Comparison with decadal climate variability in the North Pacific, as represented by the Pacific Decadal Oscillation index (1900–1997), indicates that several of the largest decadal-scale SST variations at Rarotonga are coherent with SST regime shifts in the North Pacific. This hemispheric symmetry suggests that tropical forcing may be an important factor in at least some of the decadal variability observed in the Pacific Ocean.

It is now recognized that significant tropical and subtropical Pacific ocean-atmosphere variability occurs on decadal-to-interdecadal time scales. However, in order to evaluate decadal-scale climate variability over time, climate records long enough to capture multiple decadal periods are needed, and these records are limited (*1*, *2*). In the North Pacific, sufficient instrumental climatic data exist to identify a pattern of irregular decadal-to-interdecadal ocean-atmosphere climate variability over the past ~100 years (*2*–*7*). The time history of the leading eigenvector of North Pacific SST back to 1900 A.D. has been termed the Pacific Decadal Oscillation (PDO) by Mantua *et al.*, (*6*). The PDO is a recurring pattern of ocean-atmosphere variability in which the central gyre cools at the same time as the eastern margin warms, or vice versa. Alternating phases of the PDO can last for two to three decades, with reversals being noted in 1924/25, 1946/47, and 1976/77 (*6*). Before 1900, little is known about decadal variability in the North Pacific. In the South Pacific, oceanographic data are extremely sparse. However, the limited data indicate that the subtropical South Pacific may also play a role in decadal-scale oceanographic variability in the Pacific (*8*–*11*). For example, the South Pacific is currently the dominant (50 to 75%) source region for isopycnal water transport to the equatorial thermocline (*10*, *11*). This is due in part to the partial blocking effect of the surface ocean beneath the Intertropical Convergence Zone (ITCZ) in the North Pacific and the more limited influence of the South Pacific Convergence Zone (SPCZ) on South Pacific isopycnal equatorward flow (*8*, *11*).

The spatial pattern of decadal variability in Pacific SSTs is similar to that associated with El Niño–Southern Oscillation (ENSO), but with lower amplitude in the tropics and higher amplitude outside the tropics (*3*, *12*). Some studies suggest that this decadal variability may originate in the subtropics of the North Pacific Ocean through unstable ocean-atmosphere interactions (*2*, *13*), whereas other studies suggest that tropical ENSO forcing plays a key role (*3*, *12*, *14*, *15*). However, several key questions regarding the nature of Pacific decadal variability remain, including the recurrence period of decadal changes in SST; whether the decadal-scale SST variability in the subtropical South Pacific is in phase with the North Pacific; and

[1]Department of Earth and Atmospheric Sciences, ES 351, University at Albany–State University of New York, Albany, NY 12222, USA. [2]Department of Biology and Biochemistry, University of Houston, Houston, TX 77204, USA. [3]Laboratory for Geochemical Oceanography, Department of Earth and Planetary Sciences, Harvard University, Cambridge, MA 02138, USA.

whether the decadal SST variability is periodic or more concentrated during certain times, such as in the late 19th and 20th centuries.

To examine decadal variability in the South Pacific, we produced a proxy record of SST from a coral growing at Rarotonga. The island of Rarotonga is located at 21.5°S and 159.5°W in the Cook Islands in the region of the eastern SPCZ. Corals growing at Rarotonga are exposed to open ocean conditions of the westward flowing South Equatorial Current. SST in the 2°-by-2° grid surrounding Rarotonga averages 25.7°C, with a consistent 4° to 5°C seasonal SST range, with maximum water temperatures occurring in February-March of each year (*16*). This region has also been identified as a "center of action" for monitoring changes in the Southern Oscillation (*17*). During ENSO "warm mode" (El Niño) events, the SPCZ moves to the northeast, joining the ITCZ in the central-western tropical Pacific. This condition leads to cooler and drier than average conditions in the region. During ENSO "cool modes" (or La Niña conditions), the situation reverses, SST rises, and the SPCZ intensifies.

In April 1997, 3.5 m of continuous coral core (representing 271 years of growth) (*18*) was collected by hydraulic drill from a massive colony of *Porites lutea* in 18.3 m of water on the southwest side of Rarotonga at 21°14′11″S, 159°49′59″W. We measured Sr/Ca on 1-mm-interval samples spanning the entire core and measured oxygen isotopes ($\delta^{18}O$) over the intervals from 1950 to 1997 (at 1 mm resolution) and 1726 to 1770 (at 2 mm resolution) for calibration purposes (*19–21*). Over the interval from 1981 to 1997, both Sr/Ca and $\delta^{18}O$ were compared to instrumental SST from the Integrated Global Ocean Service System Products (IGOSS) data (*16*) in the 1°-by-1° grid centered at 22°S and 160°W. The Sr/Ca data show a remarkable coherence with SST over seasonal and interannual time scales, with a seasonal amplitude consistent with the average annual SST cycle of 4° to 5°C (Fig. 1). For $\delta^{18}O$ (*22*), the seasonal range of ~0.9 to 1.0 per mil (‰) matches the expected range if water temperature was the dominant influence on coral $\delta^{18}O$ (*23*). However, there are also intervals where $\delta^{18}O$ does not track SST very well. Linear least-squares regression analysis indicates that the variability in Sr/Ca explains significantly more of the variance in SST ($r^2 = 0.75$) than does coral $\delta^{18}O$ ($r^2 = 0.54$) (*24*). This is not surprising, because we expect coral skeletal $\delta^{18}O$ to be affected by both SST and $\delta^{18}O_{seawater}$, whereas skeletal Sr/Ca has been shown to vary with SST alone (*25*).

The derived relation between SST and Rarotonga coral Sr/Ca is [SST (°C) = 140.55 – 12.15(Sr/Ca × 1000)]. The slope of this regression equation is similar to that determined for coral calibrations at other locations (*25–28*). Considering that IGOSS SST values represent a 1°-by-1° grid centered at 22°S, 160°W, whereas the Sr/Ca data represent a single point from 18 m depth at Rarotonga, the high degree of correlation obtained is remarkable and demonstrates the utility of Sr/Ca as a proxy for SST at this location.

To determine whether interannual and decadal Sr/Ca variations are also the result of SST changes, we compared Sr/Ca-derived SST anomalies to instrumental SST anomalies for the period from 1950 to 1997 (Fig. 2). Both interannual and decadal changes in coral Sr/Ca-derived SST anomalies are significantly correlated with instrumental SST anomalies, particularly back to 1960, which includes the most continuous part of the instrumental SST record (*29*). Most El Niño events are recorded as cool anomalies at Rarotonga but with reduced amplitudes as compared to the tropical Niño3/4 region (*30*). Although not shown here, it is noteworthy that decadal changes in coral $\delta^{18}O$ at Rarotonga do not closely track SST and coral Sr/Ca, possibly indicating the effects of decadal changes in the $\delta^{18}O$ composition of seawater and/or salinity on coral $\delta^{18}O$ at this site.

The complete Sr/Ca-derived SST record back to 1726 shows variability over a range of time scales (Fig. 3). SSTs have varied between 23° and 24°C in the winter to 27° to 28°C in the summer from 1997 back to 1765, with pronounced interannual and decadal variations. From 1726 to 1765, mean annual SST was ~1° to 1.5°C higher, with the same seasonal amplitude. Because this excursion is so unusual, we tested the reliability of the Sr/Ca data by measuring $\delta^{18}O$ over the same interval. The $\delta^{18}O$ data show a 0.3‰ excursion equivalent to the SST change indicated by the Sr/Ca data. This suggests that a large SST shift in the central South Pacific gyre did occur at this time, although this conclusion should be confirmed with additional coral records. A mid-1700s warm interval has not been found in other

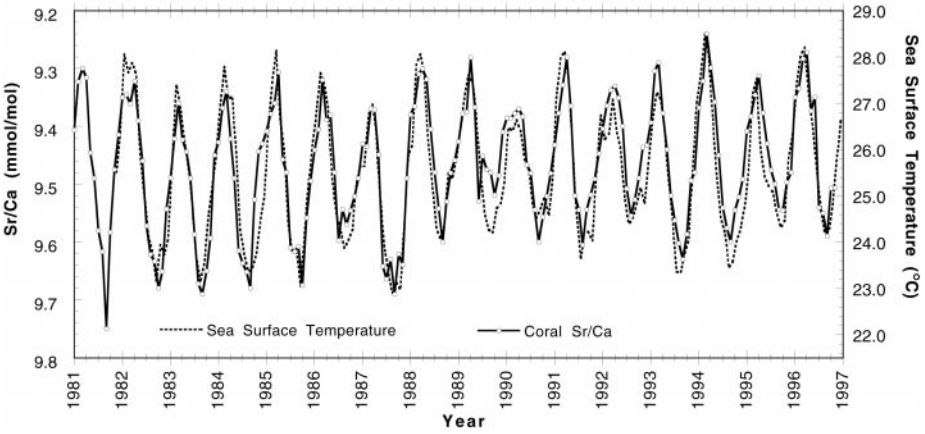

Fig. 1. Comparison of monthly IGOSS SST (*16*) for the grid including Rarotonga (1° by 1°; centered at 22°S, 160°W) and near-monthly Rarotonga coral Sr/Ca, spanning the interval from 1981 to 1997. The linear least-squares correlation between SST data and Rarotonga Sr/Ca has an $r^2 = 0.75$ (*24*).

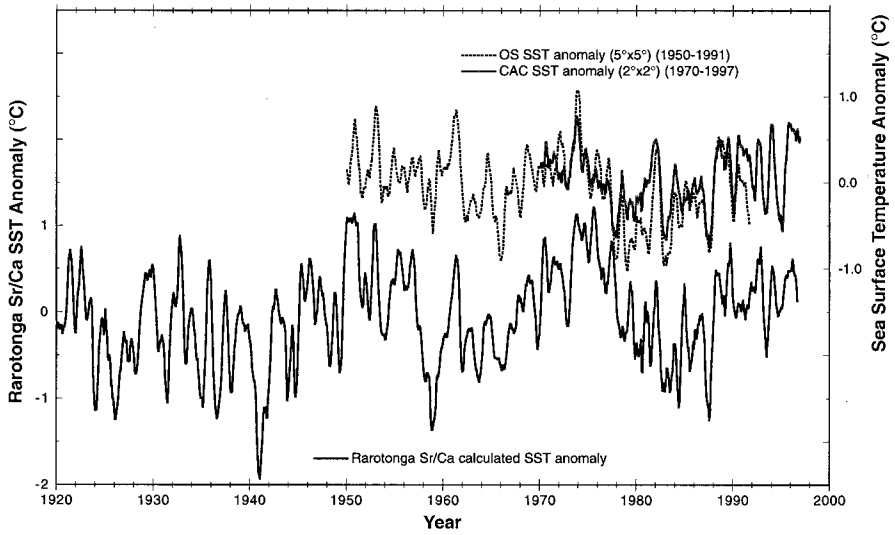

Fig. 2. Comparison of Rarotonga Sr/Ca-calculated SST anomalies (deseasonalized) with instrumental SST from a grid measuring 2° by 2° (CAC SST anomalies) and 5° by 5° (OS SST anomalies) for the Rarotonga region (*29*).

paleoclimatic records from the subtropical South Pacific, but none of these records are from the central gyre region. After the abrupt 1.5°C cooling from 1764 to 1766, the Sr/Ca series records a gradual 0.75°C cooling to ~1910 and then gradual 0.5°C warming to the present.

In comparison to equatorial areas of the central Pacific, decadal and interdecadal variance in Rarotonga coral Sr/Ca is relatively large in relation to variance attributed to interannual variability (*31*). This observation is in agreement with what is known about SST variability in the North and South Pacific gyres, based on historical measurements (*3*, *12*). As recorded at Rarotonga, the mean recurrence period of the irregular, broad-band, decadal SST variability is near 14 years, with a total of 11 decadal intervals in which mean annual water temperatures cooled by >0.75°C: 1976–77, 1956–58, 1922–1940, 1903–06, 1871–75, 1841–44, 1829–37, 1820–23, 1788–92, 1764–66, and 1756–1759 (Fig. 4). A decadal mode of variability is also found in the multicentury $\delta^{18}O$ coral record from New Caledonia, located in the western South Pacific south of the SPCZ (*32*). However, this decadal variability is not coherent with the Rarotonga Sr/Ca record. Perhaps this is due to the different climate regime at New Caledonia as compared to the central gyre location of Rarotonga. The abrupt 0.6°C cooling event that occurred in 1815, with a gradual warming until 1819, may be related to the Tambora eruption in April 1815 (*33*–*35*). The stratospheric dust veil produced by this eruption is known to have lowered temperatures in Europe and North America for several years after the eruption. The 0.5°C cooling observed at Rarotonga is also in agreement with reports of a comparable cooling in the tropics (*35*) and as found in other coral records (*36*, *37*).

To examine whether the decadal-scale SST changes inferred from the Rarotonga coral are consistent with what is known about decadal-scale variability in the subtropical North Pacific, in Fig. 4 we compare the Rarotonga Sr/Ca-derived SST record to the PDO index. Mantua *et al.* (*6*) formulated the PDO index so that when the central North Pacific is cooler than average and the Gulf of Alaska and the waters along the Pacific Coast of North America are warmer than average, the index is positive. These periods tend to correspond with times of increased frequencies of ENSO warm phases. Increased frequencies of La Niña years correspond with the negative phase of the index, when the central North Pacific is warmer than average, and the coastal waters of the NE Pacific are cooler than average. Over the past century, several of the most pronounced decadal changes in the PDO index (1976–77, 1956–58, 1945–47) are evident in the Rarotonga Sr/Ca record as well as other more subtle changes in Rarotonga SST (see 1915–40). Times of disagreement around 1910 and the early 1960s may be related to the fact that we are comparing a specific point in the South Pacific with a North Pacific–wide index. Cross-spectral analysis of Rarotonga Sr/Ca and the PDO indicates that the Rarotonga Sr/Ca record is moderately coherent with the PDO index at a decadal period centered near 15 years and at an interannual ENSO period near 6 years (80% confidence level) (*38*). The degree of correlation is hampered by the short section of overlap (97 years) in relation to the long period of the decadal-scale changes. Longer records from the North Pacific would allow a more rigorous evaluation of the extent of coherence of decadal SST variability about the equator.

The fact that several of the largest decadal changes observed in the past 100 years are in phase in the North and South Pacific gyres suggests that the origin of the decadal variability during these times of coherent behavior is likely to lie in the tropics, which is consistent with some previous suggestions (*3*, *12*, *14*, *15*). The specific mechanism could be the export

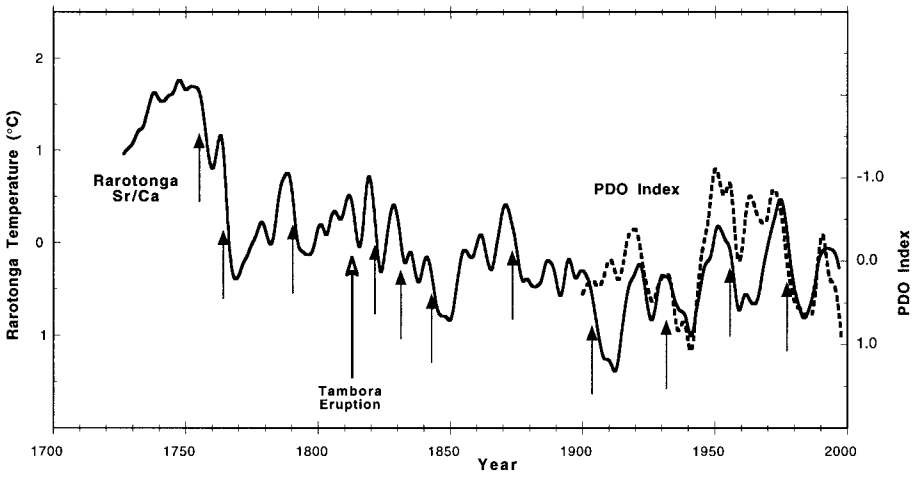

Fig. 4. Comparison of 8-year low-pass–filtered versions of Rarotonga Sr/Ca-calculated SST with the mean removed (solid line) and the PDO index (dashed line). As defined by Mantua *et al.* (*6*), a positive phase of the PDO index corresponds to a El Niño mode, and a negative phase corresponds to a La Niña mode. Solid arrows denote decadal cooling shifts of >0.75°C at Rarotonga, and the open arrow indicates a cooling trend, possibly related to the Tambora eruption in April 1815.

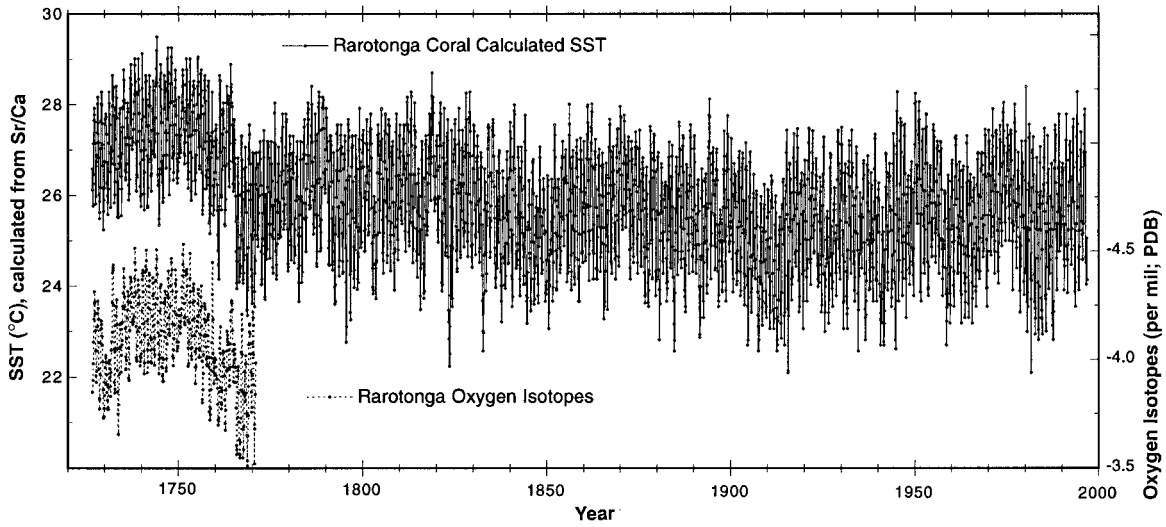

Fig. 3. (Upper curve) Near-monthly changes in calculated SST spanning 1726 to 1997, using Rarotonga coral Sr/Ca and the regression relationship [SST = 140.55 − 12.15(Sr/Ca × 1000)] derived using data shown in Fig. 1. (Lower curve) $\delta^{18}O$ measurements spanning the interval from 1726 to 1770.

and subtropical amplification of a decadal mode of ENSO from the tropics to the subtropics. However, as discussed in (*12*), different spatial patterns of midlatitude atmospheric circulation anomalies for ENSO-band and decadal variability suggest that different tropical forcing mechanisms are involved on these two time scales. Thus, the specific mechanism for generating subtropical decadal SST variability in the Pacific gyres appears to be complex and may involve tropical-subtropical ocean-atmosphere interactions other than ENSO.

References and Notes

1. K. E. Trenberth, *Bull. Am. Meteorol. Soc.* **71**, 988 (1990).
2. M. Latif, T. P. Barnett, *Science* **266**, 634 (1994).
3. Y. Zhang, J. M. Wallace, D. S. Battisti, *J. Clim.* **10**, 1004 (1997).
4. C. Deser, M. A. Alexander, M. S. Timlin, *J. Clim.* **9**, 1840 (1996).
5. S. Minobe, *Res. Lett.* **24**, 638 (1997).
6. N. J. Mantua, S. R. Hare, Y. Zhang, J. M. Wallace, R. C. Francis, *Bull. Am. Meteorol. Soc.* **78**, 1069 (1997).
7. A. Gershunov, T. P. Barnett, D. R. Cayan, *Eos Trans. AGU* **80**, 25 (1999).
8. W. B. White, D. R. Cayan, *J. Geophys. Res.* **103**, 21335 (1998).
9. R. G. Peterson, W. B. White, *J. Geophys. Res.* **103**, 24573 (1998).
10. M. Tsuchiya *et al.*, *Prog. Oceanogr.* **23**, 101 (1989).
11. G. C. Johnson, M. J. McPhaden, *J. Phys. Oceanogr.* **29**, 3073 (1999).
12. R. D. Garreaud, D. S. Battisti, *J. Clim.* **12**, 2113 (1999).
13. N. E. Graham, *Clim. Dyn.* **10**, 135 (1994).
14. G. A. Jacobs *et al.*, *Nature* **370**, 360 (1994).
15. K. E. Trenberth, J. W. Hurrell, *Clim. Dyn.* **9**, 303 (1994).
16. R. W. Reynolds, T. M. Smith, *J. Clim.* **7**, 929 (1994).
17. K. E. Trenberth, in *Teleconnections Linking Worldwide Climate Anomalies*, M. H. Glantz, R. W. Katz, N. Nicholls, Eds. (Cambridge Univ. Press, 1991), pp. 13–42.
18. We cut 7-mm-thick slabs of coral, which were cleaned in deionized water in an ultrasonic bath. Dry slabs were sampled with a low-speed microdrill along tracks parallel to corallite traces, as identified in x-ray positives, with a round diamond drill bit 1 mm in diameter.
19. We used an inductively coupled plasma atomic emission spectrophotometer at Harvard University to measure coral skeletal Sr/Ca, following a technique described in detail by D. P. Schrag [*Paleoceanography* **14**, 97 (1999)]. The external precision was better than 0.15% (relative standard deviation), based on analyses of replicate samples.
20. We measured oxygen isotopes on a gas source mass spectrometer with an individual acid reaction vessel system, following procedures outlined by B. K. Linsley, L. Ren, R. B. Dunbar, and S. S. Howe [*Paleoceanography* **15**, 322 (2000)]. External precision was better than 0.04‰ for $\delta^{18}O$, based on analyses of replicate samples.
21. To construct the chronology, we tied the annual minima in Sr/Ca and $\delta^{18}O$ to February (on average the warmest month) and maximum Sr/Ca and $\delta^{18}O$ to August/September (on average the coolest months). We also assumed that density bands in this coral skeleton are deposited annually.
22. B. K. Linsley, G. M. Wellington, D. P. Schrag, data not shown.
23. G. M. Wellington, R. B. Dunbar, G. Merlen, *Paleoceanography* **11**, 467 (1996).
24. Three-month running averages result in correlations to IGOSS SST of $r^2 = 0.82$ for Sr/Ca and $r^2 = 0.59$ for $\delta^{18}O$. We believe that the 3-month running average regression results may be more representative of the actual relation with SST, because the age model for the coral record may have uncertainties of 1 to 2 months.
25. J. W. Beck *et al.*, *Science* **257**, 644 (1992).
26. S. de Villiers, G. T. Shen, B. K. Nelson, *Geochim. Cosmochim. Acta* **58**, 197 (1994).
27. C.-C. Shen *et al.*, *Geochim. Cosmochim. Acta.* **60**, 3849 (1996).
28. C. Alibert, M. T. McMulloch, *Paleoceanography* **12**, 345 (1997).
29. Evaluation of the Comprehensive Ocean Atmosphere Data Set SST data for the 2°-by-2° region around Rarotonga reveals that near-continuous monthly data exist only back to 1960. The Global Ocean Surface Temperature Atlas data for the 5°-by-5° region around Rarotonga only contain near-continuous SST anomaly data back to 1950. Both SST databases contain virtually no measurements before 1930. Thus, we compared interannual and decadal changes in Sr/Ca to measured SST anomalies only back to 1950. The Climate Analysis Center (CAC) SST anomalies are from (*16*). The optimally smoothed (OS) SST anomaly data are from Kaplan *et al.* [*J. Geophys. Res.* **103**, 18567 (1998)]. Correlations between annually averaged coral Sr/Ca and annually averaged OS SST and CAC SST anomalies have r^2 values of 0.45 and 0.37, respectively. Although these are lower than the correlation to 1°-by-1° IGOSS SST, they are both significant at the 99% level.
30. The Niño3/4 SST record reflects SST anomalies in the central equatorial Pacific region bounded by 5°S–5°N and 120°–170°W.
31. This observation is based on Singular Spectrum Analysis (SSA) of the Sr/Ca Series (1726–1997), using software written by E. Cook (Lamont-Doherty Earth Observatory). After bandpass filtering to remove the annual cycle and periods greater than 50 years, 37% of the variance is attributed to decadal and interdecadal variability and 43% of the variance to ENSO band (3- to 7-year) variability ($n = 3244$ and window length = 120 months). In comparison, SST variability in the equatorial Nino3/4 region contains only 18% of variance in the decadal and interdecadal bands and 64% in the interannual band [based on the same SSA analysis of Kaplan OS SST anomaly data (*29*) for the Nino 3/4 region].
32. T. M. Quinn *et al.*, *Paleoceanography* **13**, 412 (1998).
33. M. R. Rampino, S. Self, *Quat. Res.* **18**, 127 (1982).
34. R. B. Stothers, *Science* **224**, 1191 (1984).
35. H. H. Lamb, *Philos. Trans. R. Soc. London Ser. A* **266**, 425 (1970).
36. T. J. Crowley, T. M. Quinn, F. W. Taylor, C. Henin, P. Joannot, *Paleoceanography* **12**, 633 (1997).
37. J. E. Cole, R. B. Dunbar, T. R. McClanahan, N. Muthiga, *Science* **287**, 617 (2000).
38. Cross-spectral analysis was done on 2-year low-bandpass–filtered versions of Rarotonga Sr/Ca and the PDO with the ARAND software package, which is maintained and distributed by P. Howell of Brown University.

39. We thank O. Hoegh-Guldberg and J. Caselle for assistance with field sampling and E. Goddard and S. Howe for analytical assistance. Comments from two anonymous reviewers were also greatly appreciated. Supported by NSF grant ATM-9901649 and NOAA grant NA96GP0406 to B.K.L., NSF grant ATM-9619035 and NOAA grant NA96GP0470 to G.M.W., and NSF grants OCE-9733688 and OCE-9819257 to D.P.S.

8 June 2000; accepted 10 October 2000

Contributions of Land-Use History to Carbon Accumulation in U.S. Forests

John P. Caspersen,[1]* Stephen W. Pacala,[1] Jennifer C. Jenkins,[2] George C. Hurtt,[3] Paul R. Moorcroft,[1] Richard A. Birdsey[4]

Carbon accumulation in forests has been attributed to historical changes in land use and the enhancement of tree growth by CO_2 fertilization, N deposition, and climate change. The relative contribution of land use and growth enhancement is estimated by using inventory data from five states spanning a latitudinal gradient in the eastern United States. Land use is the dominant factor governing the rate of carbon accumulation in these states, with growth enhancement contributing far less than previously reported. The estimated fraction of aboveground net ecosystem production due to growth enhancement is 2.0 ± 4.4%, with the remainder due to land use.

Although mid-latitude forests of the northern hemisphere are known to provide a large sink for atmospheric CO_2 (*1*–*3*), considerable uncertainty remains about the cause of the sink. Nitrogen deposition, CO_2 fertilization, and climate change have been shown to enhance tree growth in forest ecosystems (*4*), but historical changes in land use also provide an alternative explanation for the sink, particularly the regrowth of forests after agricultural abandonment, reduced harvesting, and fire suppression (*5*). Assessing the relative contribution of land use and growth enhancement is critical for planning strategies to mitigate the accumulation of CO_2 in the atmosphere (*6*). If forests are simply regrowing in response to changes in land use, then the sink can be expected to saturate as forests regain their former biomass. However, if tree growth has been enhanced, then the future storage potential of forests is much less certain.

Estimates of the fraction of the forest sink due to regrowth versus enhancement vary widely, but growth enhancement has been consistently estimated to be large. In the United

[1]Department of Ecology and Evolutionary Biology, Princeton University, Princeton, NJ 08540, USA. [2]Northeastern Research Station, USDA Forest Service, Post Office Box 968, Burlington, VT 05402, USA. [3]Complex Systems Research Center, Institute for the Study of Earth, Oceans, and Space, University of New Hampshire, Durham, NH 03824, USA. [4]Northeastern Research Station, USDA Forest Service, 11 Campus Boulevard, Suite 200, Newtown Square, PA 19073, USA.

*To whom correspondence should be addressed. E-mail: jpc@eno.princeton.edu